Aviation Technology, Integration, and Operations Conference, 16-20 June 2014, Atlanta, Georgia

Conceptual Design of the Joby S2 Electric VTOL PAV

Alex M. Stoll[*], JoeBen Bevirt[†], Percy P. Pei[‡], and Edward V. Stilson[§]

Joby Aviation, Santa Cruz, California, 95060

Recent advances in electric propulsion technologies have opened up new design options for aircraft through the application of distributed electric propulsion. Notably, many vertical takeoff and landing configurations that were previously impractical or impossible now have the potential to become viable aircraft that provide transformational capabilities. One such configuration, a two-seat fully-electric 200 mph personal aircraft with 200 mile range, is being designed by Joby Aviation to meet unaddressed commuting and transportation desires. The distributed nature of the propulsion system enables unprecedented redundancy and simplicity in a VTOL aircraft, resulting in increased safety and lower maintenance; additionally, other aspects of this configuration reduce noise signatures and drastically decrease energy usage, and the 200 mph cruise speed is significantly faster than comparable existing small VTOL aircraft. Design goals are introduced to constrain the design space to practical and viable configurations. The conceptual design of this aircraft entailed the use of design tools of various fidelity, including vortex-lattice analysis, blade-element momentum theory codes, and full Navier-Stokes CFD analysis. A sizing code integrated results from these tools along with semi-empirical mass estimates to perform mission analysis and analyze trade-offs between various design variables. The resulting aircraft design demonstrates the potential of these new electric propulsion technologies to enable viable and attractive new VTOL configurations that can provide new capabilities to private pilots.

Nomenclature

A_d	drag area of the aircraft minus the wing
AR	wing aspect ratio
C_L	lift coefficient
C_{D_0}	wing lift-independent drag coefficient
C_{L_0}	lift coefficient that minimizes lift-dependent parasitic drag
e	span efficiency
k	lift-dependent parasitic drag factor
L/D	lift-to-drag ratio
S	wing planform area

I. Introduction

Although vertical takeoff and landing (VTOL) aircraft have been in operation for many decades, their limitations have constrained their application to certain niches. For example, the most prolific VTOL configuration for transportation is the helicopter, but existing helicopter designs are significantly compromised in cruise speed and efficiency (about 3-4 times lower L/D than equivalent fixed-wing aircraft,[1] which reduces range and increases operating costs), and their large noise signatures limit their operation within populated areas.[2] However, recent advances in electric propulsion technology have created the potential for new VTOL

*Aeronautical Engineer, 340 Woodpecker Ridge, AIAA Member.

†Founder, 340 Woodpecker Ridge.

‡Structural Engineer, 340 Woodpecker Ridge.

§Composites Engineer, 340 Woodpecker Ridge.

configurations that have not been practical with a traditional combustion engine architecture. This is due to the relatively scale-free nature of electric motors, which allows the use of a relatively large number of smaller motors placed in strategic locations around the aircraft without the great increase in complexity and weight that would accompany the use of a similar number of independent combustion engines and/or gearboxes and driveshafts. Although the specific energy of contemporary batteries is not high enough for practical long-range VTOL aircraft, a practical medium-range VTOL aircraft utilizing distributed electric propulsion to address the noise, speed, and efficiency compromises of helicopters has been designed. In addition to noise and efficiency improvements, electric propulsion can result in lower maintenance and increased reliability, further reducing operating costs and increasing safety due to lower chances of mechanical failures. Safety also can be improved through distributed electric propulsion, which offers the potential for a highly-redundant propulsion system.

II. Design Goals

The goal of this design effort is to take advantage of recent advances in technology to create a truly transformative vehicle for commuting and traveling short to medium distances in the form of a fast, safe, quiet, and efficient two-seat VTOL aircraft. To facilitate operation within cities on larger scales than current helicopter operations, noise levels must be drastically reduced and safety levels must be increased relative to current state of the art small helicopters. These qualities also directly increase attractiveness to pilots and passengers. For this to be a practical aircraft, range and cruise speed must be adequately high; design goals are 200 miles at 200 mph, with a 45-minute reserve, as required by FAA federal aviation regulations (FARs) for instrument flight rules flight. This provides a significant increase in speed relative to comparable contemporary VTOL aircraft; for example, the Robinson R22 helicopter cruises at 110 mph.[3] The cruise altitude is chosen as 12,000 feet, an altitude low enough not to require supplemental oxygen (as stipulated by FAR requirements). Side-by-side seating is selected to provide a more attractive environment for the occupants compared to a tandem configuration.

III. Configuration Description

Because the relatively scale-free nature of electric propulsion enables the use of a large number of smaller motors distributed across the airframe, a distributed electric propulsion configuration was adopted chiefly to increase safety during VTOL operations through redundancy. Twelve individual motors each drive a single fixed-pitch propeller; these motors are mounted on linkages that tilt the motors and propellers between vertical and horizontal orientations during the transition between vertical and horizontal flight, in what is effectively a distributed tilt-rotor architecture. The use of multiple individual tilt linkages eliminates the single point of failure present in tilt-wing designs. These propellers are only used during takeoff and landing, and their blades are able to fold such that, when folded, they lie flat against nacelles, minimizing their drag impact in cruise. The folding hinges also act as flapping hinges to react unsteady blade loads and reduce structural demands on the blades and the hubs. These propellers are designed for low tip speeds (nominally 390 ft/s) to significantly reduce the noise signature during takeoff and landing. An additional benefit of this configuration is the increased dynamic pressure over the wing during transition due to the velocity induced by the propellers, providing an effective high-lift device; as a result, the wing area can be reduced for a given stall speed constraint, and the increased wing loading provides cruise drag and ride quality benefits.[4]

The propellers are spatially distributed around the aircraft by positioning them along the leading edges of the wing and tail, with eight mounted on the wing and four on the tail. This longitudinal and lateral distribution facilitates control and stability during takeoff and landing and helps to reduce the power and torque demands on the motors in the event of the loss of a single motor. High-bandwidth RPM control of the electric motors allows the use of rotational speed to modulate thrust for stability and control in VTOL and precludes the need for complex collective or cyclic blade pitch adjustment mechanisms.

Propulsion in cruise is accomplished by a separate set of cruise-optimized fixed-pitch propellers. A pair of these cruise propellers are mounted on the wingtips and take advantage of the wingtip vortices to improve propulsive efficiency.[5] Scrubbing drag is also greatly reduced compared to conventional fuselage-mounted tractor propeller configurations. All of the propellers are driven by custom-designed high-performance brushless electric motors, and powered by lithium-ion batteries.

Because the center of gravity location is constrained by the VTOL propeller locations, a forward-swept wing allows the center of gravity to be located closer to the occupants, which reduces the longitudinal shift of the center of gravity between one- and two-pilot flights. Additionally, the aeroelastic twist properties of a forward-swept wing oppose the torsion resulting from the cantilevered motor masses and potentially allow for a lighter wing (pending the results of a more detailed aeroelastic analysis). The wing airfoil was chosen to minimize drag at the target cruise C_L while providing a high power factor at the reserve cruise conditions and an adequately high maximum lift coefficient, and full-span plain flaps are employed to lower stall speed during takeoff and landing.

In addition to the safety benefits of the highly redundant VTOL system, this configuration, in contrast to many VTOL aircraft, retains the ability to perform conventional takeoffs and landings on runways. This capability is useful both as a backup mode in the event of a system failure or operational constraints precluding VTOL, and as a strategy to increase range when VTOL is unneeded. To further improve safety, a ballistic recovery system is installed.

The resulting design is illustrated in figure 1.

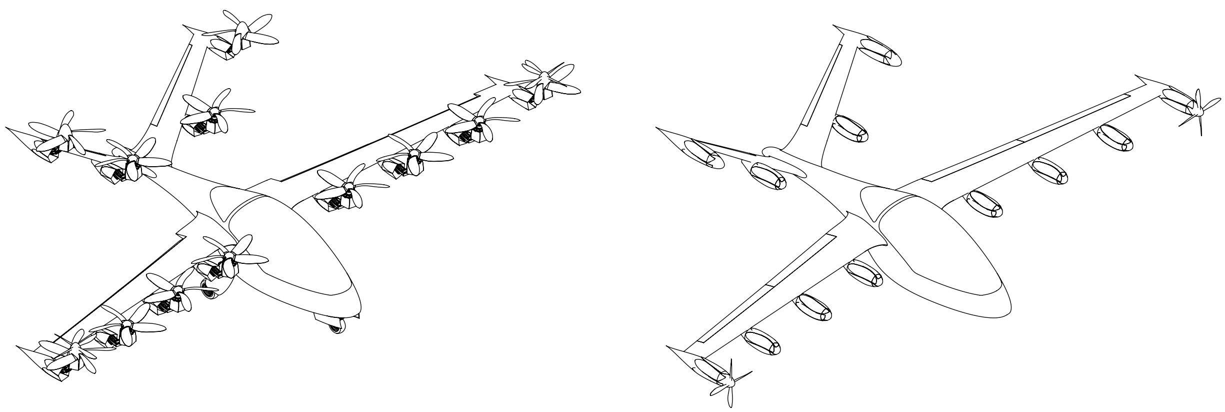

(a) VTOL configuration

(b) Cruise configuration

Figure 1. Illustration of the design in different configurations.

IV. Design and Analysis Methods

Initial configuration design was performed using XFLR5, an open-source vortex lattice code,[6] to compare the cruise efficiency (L/D) of various configurations while ensuring static and dynamic stability constraints were met. For each layout analyzed, the relative motor mass was also compared, by calculating the power and torque requirements to stabilize and control the aircraft in a worst-case single motor loss scenario. The peak power and torque requirements of the motors in this scenario strongly depend on the number and spatial distribution of the motors.

Propeller designs were initially analyzed using a custom blade-element momentum theory (BEMT) code, which employs curve fits to airfoil polars calculated by a 2D viscous panel code. Results from these analyses were fed into a time-accurate trajectory analysis code to ensure, at this level of fidelity, that a robust transition between vertical and horizontal flight is possible given the power and torque constraints, without subjecting the occupants to uncomfortable or disorienting g-forces. This code uses BEMT results for propeller performance at various advance ratios and angles of attack, and estimates the propeller induced velocity to calculate wing performance.

Extensive CFD analyses were performed on various aircraft and propeller configurations to further investigate aircraft drag and stability and propeller performance. The commercial code STAR-CCM+ was utilized for both mesh generation and CFD solutions. All CFD simulations were computed using the STAR-CCM+ unstructured, cell centered, finite volume Navier-Stokes solver. Flow turbulence was modeled using the SST (Menter) k-ω turbulence model with the γ-Re_θ transition model.

Sizing calculations were performed using semi-empirical formulations for component mass estimation. A drag polar of the form

$$C_D = C_{D_0} + \frac{C_L^2}{\pi e AR} + k(C_L - C_{L_0})^2 + A_d/S \tag{1}$$

was employed; this formulation separates the drag contributions of the wing and the remainder of the aircraft, to improve the accuracy of the sensitivity of drag to wing area. The span efficiency e was estimated from vortex-lattice analysis, with a small increase based on CFD results to account for the power savings of the wingtip propeller. The remainder of the parameters were estimated from curve fits to CFD solutions at various values of C_L, with 7.5% added to C_{D_0} and A_d as an estimate of excrescence drag not captured in the simulations. (One such CFD solution is shown in figure 2.) A sizing code using these drag and mass relations, along with propeller performance models and a mission analysis routine, allowed the effect of various design parameters to be determined. To evaluate the effect of design changes not captured by this methodology, the sizing code was executed with a different aerodynamics model using vortex lattice results along with empirical and statistical correlations to account for, e.g., fuselage effects and excrescence drag, and CFD simulations were then performed on the resulting layout to recalibrate equation 1 and analyze the stability characteristics with higher fidelity.

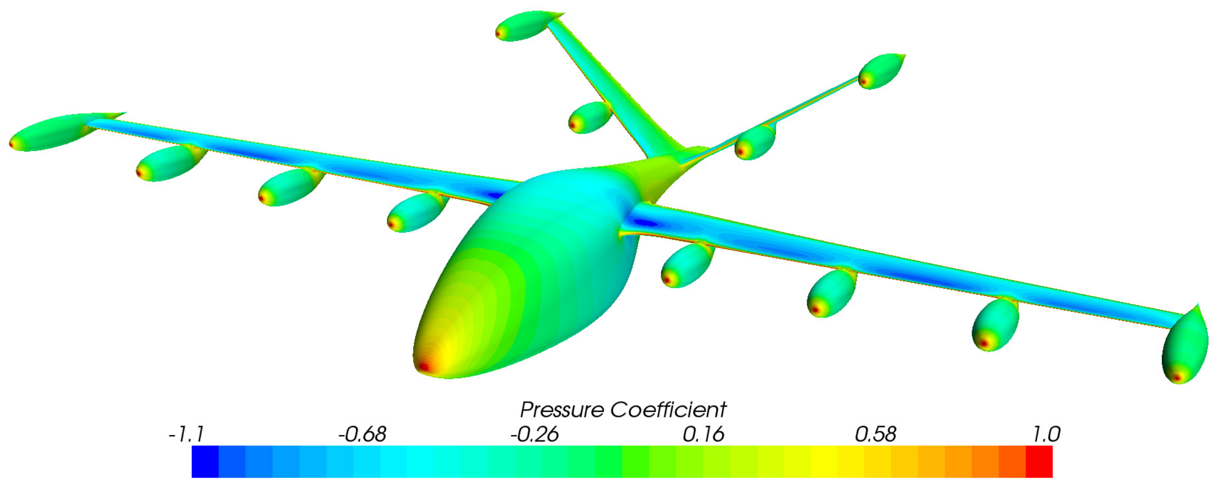

Figure 2. CFD result showing pressure coefficient contours at the cruise condition.

The folding propeller design process incorporated unusual geometric constraints to effectively nest the blades on the nacelle. The maximum twist and chord values at various radial positions along the blade were determined through CAD design of the nacelle; these constraints were then imparted into optimization software, which ran a BEMT analysis code on various blade geometries to minimize power at a specified thrust value and tip speed while meeting these geometric constraints. The initial blade geometry was determined from a BEMT design code. Propeller performance was then validated in higher fidelity at various pertinent flight conditions with CFD analysis. Various blade folding geometries were analyzed in CFD at cruise conditions; one example is shown in figure 3.

The aircraft specifications are summarized and compared with comparable existing aircraft - the Robinson R22 helicopter and the Van's RV-7 fixed wing aircraft - in table 1, and a cost comparison (utilizing estimates for energy usage and operating costs) with the Robinson R22, Van's RV-7, and Tesla Model S is given in table 2, illustrating the transformative energy and operating costs. Here, operating costs comprise insurance, energy costs, maintenance, and depreciation.

V. Conclusion

This design study underscores the potential of electric propulsion to enable new, game-changing capabilities in aircraft, notably for personal VTOL aircraft. A safe, quiet, and practical two-seat personal VTOL design was shown to be practical within the limits of the analysis undertaken; further analyses in greater detail will refine this design and pave the way for flight testing. Successful flight testing will validate the

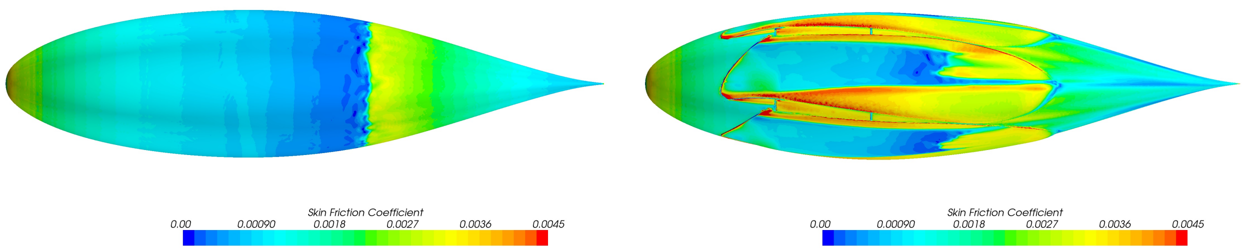

(a) Plain nacelle

(b) Nacelle with folded blades and spinner gaps

Figure 3. CFD results comparing a clean nacelle with a nacelle geometry including folding blades and spinner gaps, showing skin friction coefficient contours.

	Joby S2	Robinson R22[3]	Van's RV-7[7,8]
Seating capacity	2	2	2
Gross weight	2,000 lb	1,370 lb	1,800 lb
Maximum payload weight	390 lb	389 lb	460 lb (at max fuel)
Wing area	53.8 ft^2		121 ft^2
Wingspan	29.5 ft	25 ft (rotor diameter)	25 ft
Aspect ratio	16.2		5.2
Wing loading	37.2 lb/ft^2		14.9 lb/ft^2
Disk loading	16.3 lb/ft^2	2.61 lb/ft^2	
Cruise speed	200 mph	110 mph	199 mph
Range	200 mi	165 mi (estimated)	775 mi
Cruise C_L	0.52		0.19

Table 1. Specifications

	Joby S2	Robinson R22[9]	Van's RV-7	Tesla Model S[10]
Approximate price	$200,000	$291,700	$110,000	$100,000
Energy cost per mile	$0.05	$0.53	$0.27	$0.04
Operating cost per mile	$0.20	$1.30	$0.44	$0.15

Table 2. Comparison with the Robinson R22, Van's RV-7, and Tesla Model S at $0.12/kWh and $6.10/gallon

concept and open the doors for its application to future aircraft designs of different scales and capabilities.

References

[1] Leishman, J. G., *Principles of Helicopter Aerodynamics*, Cambridge University Press, 2006.

[2] Leverton, J. W., "Helicopter Noise: What is the Problem?" *Vertiflite*, Vol. 60, No. 2, March/April 2014.

[3] Robinson Helicopter Company, *R22 Pilot's Operating Handbook and FAA Approved Rotorcraft Flight Manual*, Oct. 1996.

[4] Kohlman, D. L., "Flight Test Results for an Advanced Technology Light Airplane," *Journal of Aircraft*, Vol. 16, No. 4, April 1979, pp. 250–255.

[5] Miranda, L. and Brennan, J., "Aerodynamic effects of wingtip-mounted propellers and turbines," *Fluid Dynamics and Co-located Conferences*, American Institute of Aeronautics and Astronautics, June 1986.

[6] Deperrois, A., "XFLR5," http://www.xflr5.com, May 2014.

[7] "Van's Aircraft - Aircraft Models: RV-7/7A Performance," http://www.vansaircraft.com/public/rv7perf.htm, June 2014.

[8] "Van's Aircraft - Aircraft Models: RV-7/7A Specifications," http://www.vansaircraft.com/public/rv7specs.htm, June 2014.

[9] Robinson Helicopter Company, *R22 Beta II - 2014 Estimated Operating Costs*, Feb. 2014.

[10] "True Cost of Ownership — Tesla Motors," http://www.teslamotors.com/true-cost-of-ownership, May 2014.